Chapter 9

Dynamics of the first-order transition in $Gd_5(Si_xGe_{1-x})_4$: cycling and avalanches

9.1 Introduction

In this chapter, we study the dynamics of the first-order magnetostructural transition in $Gd_5(Si_xGe_{1-x})_4$ alloys. Firstly, we study the effect on the entropy change, ΔS, of inducing the transition either by T or H. Secondly, we present a systematic study of the effect of cycling a sample through the first-order transition. We show the evolution of ΔS with the number of cycles and we also analyse the avalanches between metastable states of the system during the transition. All the foregoing allows to unveil the actual mechanism that drives the first-order transition in $Gd_5(Si_xGe_{1-x})_4$ alloys.

9.2 Comparison of the entropy change induced by temperature and by field

As already explained in Chapter 4, DSC are usually designed to continuously sweep temperature while $\dot{Q}(t)$ is measured. The T sweep induces thermally the first-order transition in the sample, while heat is released or absorbed. In the particular case of field-induced transitions, the temperature T_t of the peak of the transition in the calorimetric curve is tuned by the magnetic field, and consequently the field dependence of ΔS can be obtained. Besides, our DSC also works sweeping H. By fixing a temperature above $T_t(H = 0)$ and increasing the magnetic field, the first-order transition can also be induced.

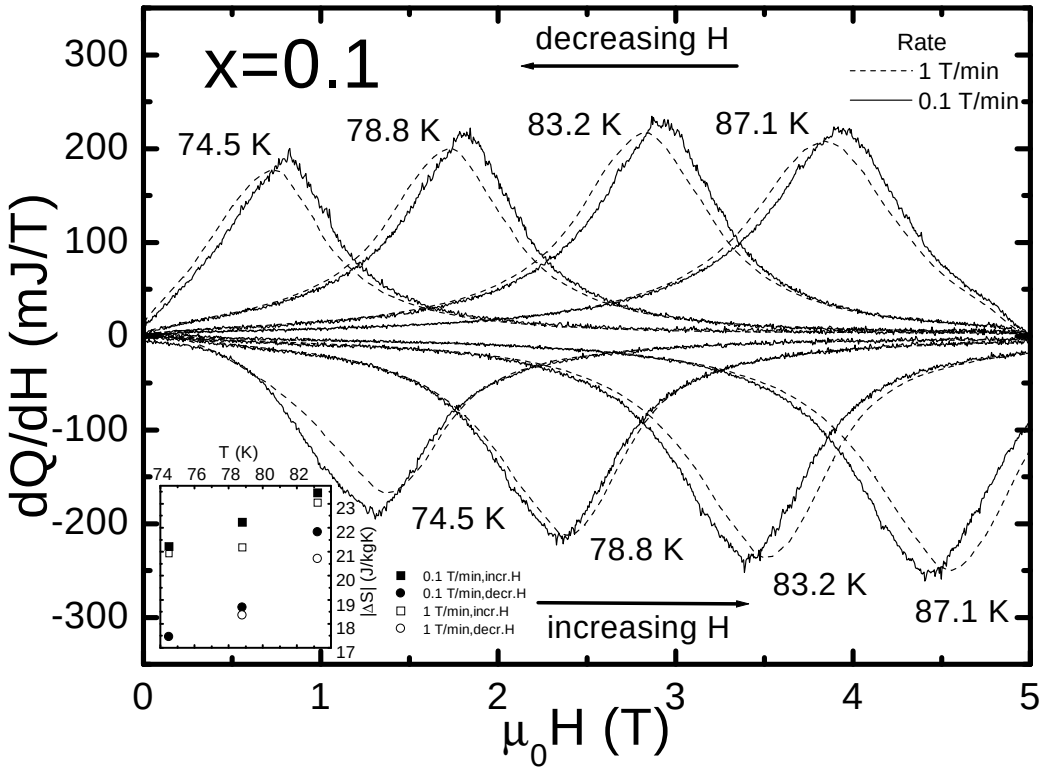

Figure 9.1: Calorimetric curves recorded sweeping the field (increasing and decreasing H) in a $Gd_5(Si_{0.1}Ge_{0.9})_4$ sample (#1, as-cast) at some fixed temperatures and for two different field rates. Inset shows the absolute value of the entropy change as a function of temperature for the different rates on increasing and decreasing H.

In order to compare the values of ΔS obtained from both processes, DSC calorimetric curves were measured sweeping the temperature and the field. DSC cuves sweeping the temperature at constant field -from now on we will call them $DSC_H(T)$-, measured for all compositions, are decribed in section 5.3. DSC data sweeping the field at constant temperature -from now on we will call them $DSC_T(H)$- were measured in the following samples: x=0.05 (#1 T4+Q), x=0.1 (#1 as-cast), x=0.3 (#2 T4+Q) and x=0.45 (#7 T4). Calorimetric curves for $DSC_T(H)$ were recorded on increasing fields up to 5 T and decreasing fields down to zero. Field rates, $\dot{H}$, of 1 and 0.1 T/min were applied. The results for x=0.05 and x=0.1 are displayed in Figs. 4.8 and 9.1, respectively. We note that ΔS does not depend on $\dot{H}$. Unfortunately, results for x=0.3 and x=0.45 cannot be used to obtain ΔS: the broadness of the transition region when the field is sweeped is too large as compared to the field range 0-5 T available in our cryostat (first-order peak cannot be integrated properly).

The values of the entropy change obtained by $DSC_H(T)$ (ΔS_H) and $DSC_T(H)$ (ΔS_T) differ in ~5 J/(kgK) for x=0.05 and ~7 J/(kgK) for x=0.1 (see Fig. 9.2). These differences are systematic in the whole temperature range in which ΔS_T is measured, and they are too high to be a consequence of the experimental error (which lies within 5-10 %).

The $H-T$ phase diagram for x=0.05 is displayed in Fig. 9.3 in order to show an example of the thermal- and field-induced processes in which ΔS_H and ΔS_T are measured. H_t and T_t values are evaluated from both DSC measurements, as well as the beginning and the ending of the transitions.

This difference can be justified using general thermodynamics [1]. The First Principle in differential form for a magnetic system is

$$dU = dQ + HdM = TdS + HdM \ , \tag{9.1}$$

where dU is the differential internal energy, dQ is the differential transfered heat and HdM is the differential external work needed to magnetise the magnetic system. The Second Principle for a reversible process, $TdS = dQ$, has been used. It is useful to work with the entalphy as the thermodynamic potential rather than the internal energy. The enthalpy, E, is defined as

$$E = U - HM \ , \tag{9.2}$$

which in differential form becomes

$$dE = dQ - MdH = TdS - MdH \ . \tag{9.3}$$

At constant field, the change in temperature from the beginning to the end of the transition leads to

$$\Delta E_H = \int TdS = Q \equiv L \ , \tag{9.4}$$

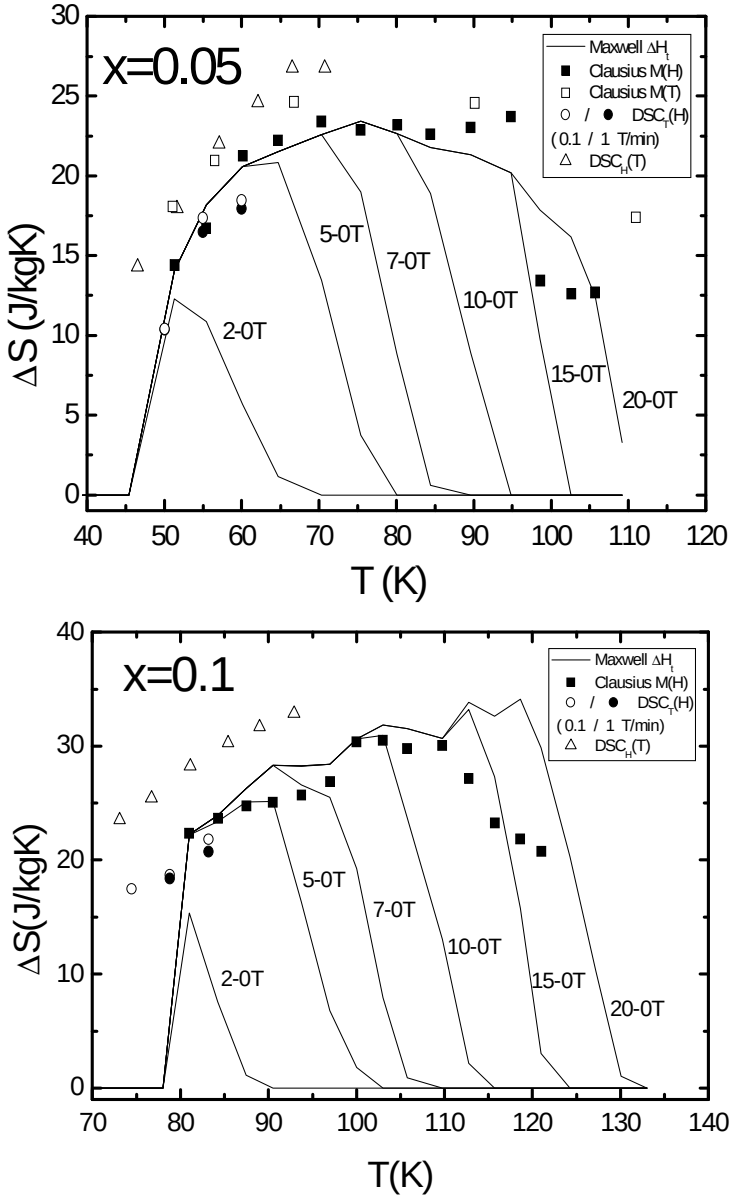

Figure 9.2: Entropy change in $Gd_5(Si_xGe_{1-x})_4$, for x=0.05 and x=0.1, calculated by using: $DSC_H(T)$ on heating (open triangles); $DSC_T(H)$ on decreasing H (open and solid circles); the Clausius-Clapeyron equation evaluated from $M(H)$ on decreasing H (solid squares); and the Maxwell relation integrating from different values of H_{max} (labeled for each curve) to zero, and evaluated only within the transition region (solid lines). For x=0.05, the entropy change calculated by using the Clausius-Clapeyron equation obtained from $M(T)$ on heating (open squares) is also displayed.

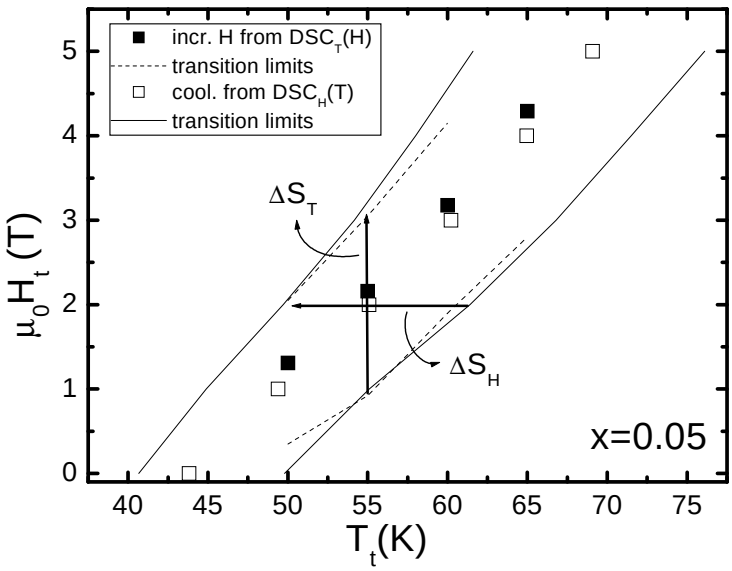

Figure 9.3: $H-T$ phase diagram for x=0.05, obtained from DSC measurements. $H_t(T)$ on increasing H (solid squares) and the corresponding starting and finishing fields of the transition (dashed lines) are obtained from DSC$_T(H)$. $T_t(H)$ on cooling (open squares) and the corresponding starting and finishing temperatures of the transition (solid lines) are obtained from DSC$_H(T)$. Examples of the processes in which the entropy change is evaluated, are labeled with arrows.

$$\Delta S_H = \int \frac{dQ}{T} = \int \frac{dE_H}{T} \ , \tag{9.5}$$

i.e., at constant field, the enthalpy change of the transition is equal to the latent heat, L, and the entropy change of the transition is calculated by integrating the differential heat divided by the temperature (Eqs. 9.4 and 9.5 are exactly the same equations as Eq. 3.10). On the other hand, if the temperature remains constant and the magnetic field varies from the beginning to the end of the transition, the enthalpy change is written as

$$\Delta E_T = Q - \int MdH = T\Delta S - \int MdH \ , \tag{9.6}$$

and therefore the latent heat and the entropy change, which are the values measured by DSC, have the following expressions:

$$Q \equiv L = \Delta E_T + \int MdH \ , \tag{9.7}$$

$$\Delta S_T = \frac{Q}{T} = \frac{\Delta E_T}{T} + \frac{1}{T}\int MdH \ . \tag{9.8}$$

In this case, the latent heat has an additional contribution to the enthalpy change due to the work of the magnetic field over the system. Since at constant temperature, the entropy change is the latent heat divided by the fixed temperature,ΔS_T has also this additional contribution.

We note that DSC measures the heat absorbed or released by the sample and therefore the entropy change is also obtained experimentally. It is straightforward to see from Eqs. 9.4 and 9.8 that ΔS obtained from $\mathrm{DSC}_H(T)$ and $\mathrm{DSC}_T(H)$ must be different. For example, when a field is applied isothermally (at T=T') in a system, changing from low to high magnetisation, it shows a negativeΔS_T. Since $(1/T)\int MdH$ is positive, the absolute value ofΔS_T will be larger than that ofΔS_H associated with a process at constant field which induces the transition on cooling at the temperature T_t=T' [1], provided that $\Delta E_T/T \approx \int dE_H/T$ [2]. The same conclusion is valid for decreasing field and heating processes. For an ideal transition, which occurs at constant field and temperature, $(1/T)\int MdH$ vanishes and both values of the entropy change are the same. We note that differences between the absolute values of ΔS_T and ΔS_H are observed in our samples. Moreover, an evaluation of $(1/T)\int MdH$ using $M(H)$ curves at the temperatures in which we have measured both ΔS_H and ΔS_T values, for x=0.05 and x=0.1, yields ~6.5 and ~8 J/(kgK), respectively. These values are in good agreement with$\Delta S_H - \Delta S_T$ (~5

[1] Figure 9.3 provides an schematic view of these two processes.

[2] This consideration is assumed *a priori*.

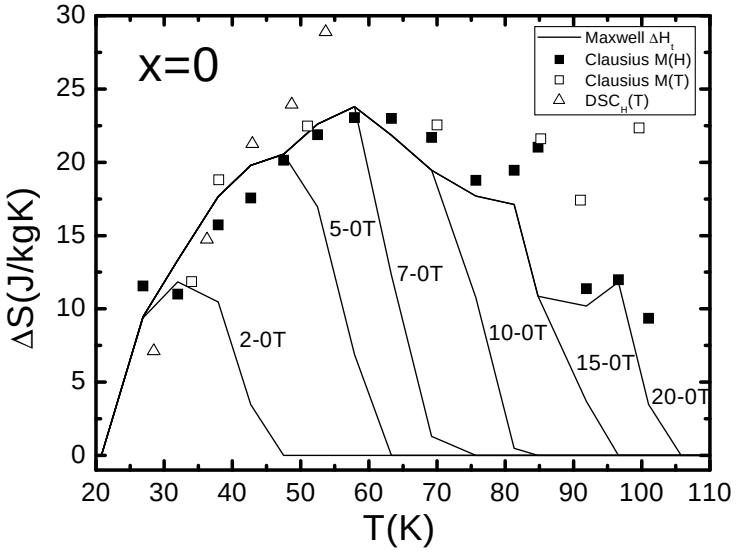

Figure 9.4: Entropy change in $Gd_5(Si_xGe_{1-x})_4$, for x=0, calculated by using: $DSC_H(T)$ on heating (open triangles); the Clausius-Clapeyron equation evaluated from $M(H)$ on decreasing H (solid squares); the Clausius-Clapeyron equation evaluated from $M(T)$ on heating (open squares); and the Maxwell relation integrating from different values of H_{max} (labeled for each curve) to zero, evaluated only within the transition region (solid lines).

J/(kgK) for x=0.05 and ~7 J/(kgK) for x=0.1), proving that these two processes are essentially different due to the work needed to magnetise the system during the transition and the validity of the approximation $\Delta E_T/T \approx \int dE_H/T$.

An indirect evaluation of the entropy change can be gained by using the Clausius-Clapeyron equation. In fact, we demonstrated in Chapter 5 that the Clausius-Clapeyron equation yields the correct value of the entropy change at a first-order transition, and for this purpose we used $M(H)$. Therefore, the entropy change actually evaluated from the Clausius-Clapeyron equation is ΔS_T. This is the reason why calorimetric measurements presented in Chapters 5 and 6 [obtained by $DSC_H(T)$] yielded larger values (it measure ΔS_H, which have been the DSC values discussed in Chapters 3-8) than those obtained with the Clausius-Clapeyron equation in some samples (see Fig. 5.9). Surprisingly, this difference decreases with increasing x. For exampe, for x=0.45 there is no difference between both values (see Fig. 5.8). This is due to the fact that $(1/T)\int MdH$ strongly decreases with temperature (both M and $1/T$ decrease with T), being $\Delta S_H - \Delta S_T \sim 1$ J/(kgK) for x=0.45, in agreement with the observed behaviour.

We also note that ΔS_T obtained from the Clausius-Clapeyron equation match the values measured by $DSC_T(H)$ (Fig. 9.2), as expected from an equivalent pro-

cess. The entropy change calculated from the Maxwell relation by integrating $M(H)$ within the transition region (see section 5.4.2), is in agreement with ΔS_T values obtained from $DSC_T(H)$ calorimetric curves as well (Fig. 9.2 for x=0.05 and x=0.1), since this evaluation arises from a field-induced isothermal process. Finally, it should also be expected that the application of the Clausius-Clapeyron equation in experimental $M(T)$ curves, *i.e.*, measurements of M at constant fields and sweeping the temperature, should yield ΔS_H. Hence, $M(T)$ curves for x=0 and x=0.05 presented in Fig. 8.5 are used to calculate indirectly ΔS_H. These values are displayed in Fig. 9.2 for x=0.05 and Fig. 9.4 for x=0. We observe that ΔS_H evaluated from $M(T)$ is larger than ΔS_T evaluated from $M(H)$, and ΔS_H values matching reasonably well with those obtained from $DSC_H(T)$.

We have shown that the entropy change when the first-order magnetostructural transition is field-induced is different than when it is thermally-induced. This relevant result is a consequence of the non-ideal behaviour of the first-order transition, since the initial and final states in the $H-T$ phase diagram (see Fig. 9.3) are different in the isothermal and the isofield processes.

9.3 Cycling through the first-order transition

Another relevant effect of the non-equilibrium dynamics of the first-order magnetostructural transition is the fact that some properties vary when the transition is repeatedly induced. In particular, changes in the resistance [2, 3] and thermopower [4] are reported for $Gd_5(Si_xGe_{1-x})_4$ alloys when they are thermally cycled through the transition.

In order to study the effect in the entropy change of cycling the transition in $Gd_5(Si_xGe_{1-x})_4$ alloys, we used three different samples (v1, v2 and v3) with x=0.05, taken from the same sample (#1 T4+Q), which were not previously used for other measurements (*virgin* samples). All samples are cut in the shape of a rod, v2 and v3 being longer than v1. We measured DSC sweeping the field[3] at a constant temperature (T=55 K) following a large number of cycles and for different field rates (within 0.01 and 1 T/min), which are summarised in Table 9.1. The first 5 cycles for sample v1, on increasing H, were measured at different $\dot{H}$ (0.01, 0.05, 0.1 and 1 T/min). Calorimetric curves scale once they are divided by $\dot{H}$, as shown in Fig. 9.5. A low $\dot{H}$ induces a low signal in the DSC sensors, which is normalised after the signal is divided by the field rate. However, the lowest $\dot{H}$=0.01 T/min appears to yield too a low signal, close to the intrinsic noise level of the measuring apparatus (see Fig. 9.5). Rates of 0.05 and 0.1 T/min yield similar shapes and almost perfectly collapse once they are normalised to $\dot{H}$,

[3] In contrast to the previous cycling studies [2, 3, 4], which used thermal cycles.

Sample	cycle #	$\dot{H}$ (T/min) incr. H	decr. H
v1	1	0.01	1
	2	0.05	1
	3,4,7,17, 21,32,43,54, 63,76,87	0.1	1
v2	1,3,4,5, 7,10,21,31	0.1	1
v3	1-12	0.1	0.1

Table 9.1: Field rates, $\dot{H}$, used for the study of the cycling through the first-order transition in the three virgin samples taken from the original x=0.05 (#1 T4+Q) sample. A given number (#) of cycle includes both an increasing and a decreasing H branch. Cycles not described in the table have a field rate of 1 T/min.

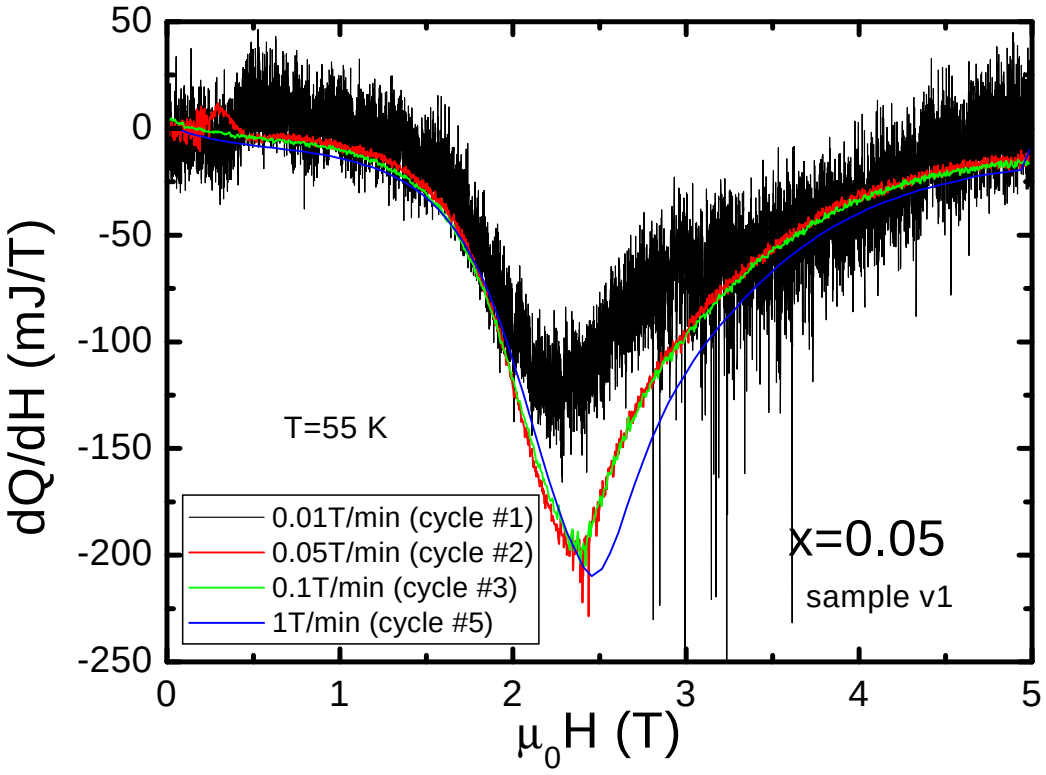

Figure 9.5: $DSC_T(H)$ curves recorded on increasing H for sample v1, at different field rates.

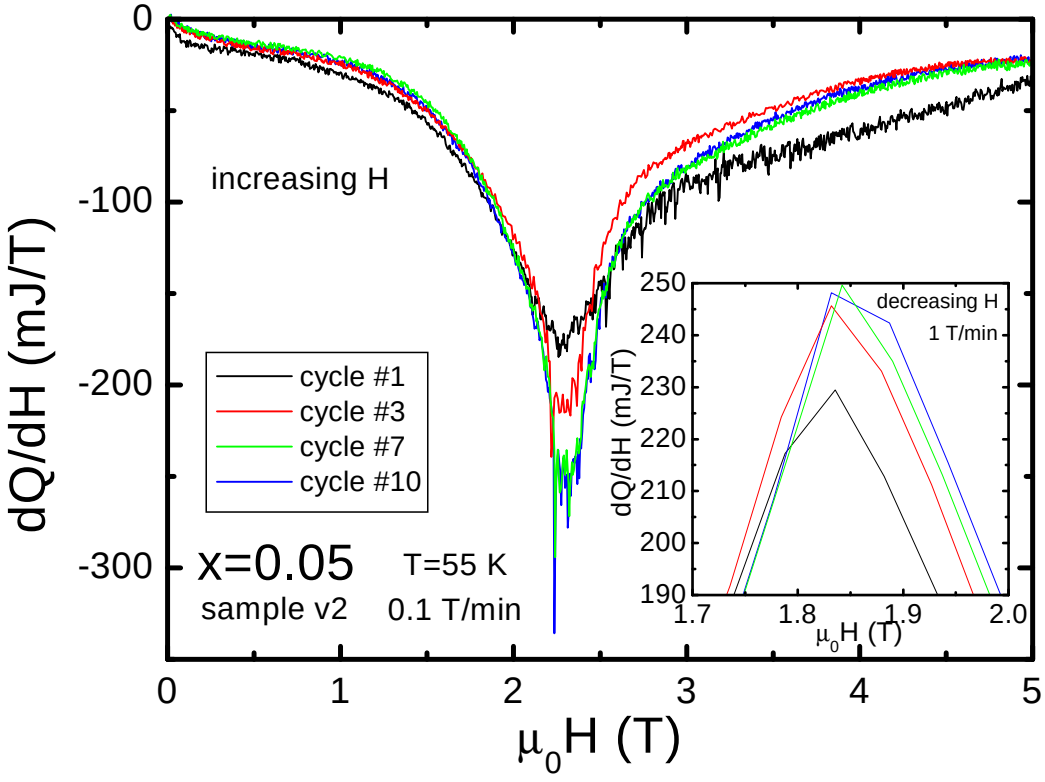

Figure 9.6: $DSC_T(H)$ curves recorded on increasing H at 0.1 T/min for different cycles in sample v2. Inset: Detail of the peak in $DSC_T(H)$ curves on decreasing H at 1 T/min following succesive cycles for sample v2.

showing an avalanche-type structure of the transition (we understand an avalanche as an irreversible jump tath makes one part of the system to undergo the transition from one phase to the other), which are completely reproducible from cycle to cycle. The fastest rate ($\dot{H}$=1 T/min) does not show avalanches, since not enough points are recorded during the phase transition to observe them.

The shape of the first DSC measurement (increasing H) for all samples is different from subsequent cycles. Even at first glance it is obvious that the first measurement enclose a lower area than the following measurements (see Fig. 9.5 for sample v1 and Fig. 9.6 for sample v2). Further measurements continue increasing in area, fact which is not directly observed in the low-rate (0.1 T/min) DSC curves, but which is appreciable in the fast-rate curves (1 T/min), as shown in the inset in Fig. 9.6. The first cycle in sample v2 (Fig. 9.6) shows small peaks of a similar size. Some of them grow, while others diminish in subsequent cycles, reaching a reproducible distribution, which is charateristic of athermal transitions (see section 9.4). The entropy change ΔS_T obtained as a function of the cycle number

is displayed for all samples in Fig. 9.7. The slight difference between the values corresponding to each sample lies within the experimental error (5-10%), which arises from the fact that part of the heat released or absorbed by the sample is not detected by the sensor. The amount of the heat losses depends on the shape of the sample. Three features observed for all samples are to be noted. Firstly, ΔS_T value increases strongly between the first and the fourth cycles, then the slope is reduced and it finally saturates before the tenth cycle. Secondly, the ΔS_T values do not depend on the field rate, even when $\dot{H}$ increases by a factor of 10. Third, values obtained from the curves on increasing H are systematically larger (in absolute value) than those obtained on decreasing H. The first result can be understood by considering that both initial and final states change from cycle to cycle due to the evolution of the disorder (for example, microcracks associated with the strain due to the continuous expansion/contraction of the crystallographic cell through the transition). When the path of the system through the first-order transition becomes reproducible, as occurs in our samples (as for example in Fig. 9.6, where the curves tend towards a reproducible pattern), then the entropy change associated with the transition reaches a constant value. In this evolution, the low-field phase disorders (the entropy increases) and/or the high-field phase orders (the entropy decreases). The non-dependence of the entropy change on $\dot{H}$ indicates that the experimental procedure is not affected by the field rate used, and that the same initial and final states are reached at any field rate. Finally, differences between the results corresponding to increasing and decreasing H appear because of hysteresis in the initial and final states, and therefore the entropy change between the two states may show slight differences.

9.4 Avalanches

The analysis of the avalanche events was also performed. Avalanches are associated with the nucleation and growth of domains of the new phase that take place during the first-order field-induced phase transition.

First-order transitions can be thermally activated or can be athermal. In the former, the relaxation from a metastable state may occur at constant external conditions due to thermal fluctuations, while in athermal transitions it occurs only under the change of an external parameter (magnetic field, stress, temperature, etc.), which modifies the difference of the free energy between the two phases [5, 6].

When a system is externally driven through a first-order phase transition, it jumps from a given configuration -which is a state corresponding to a local minimum of the free energy - towards a different configuration, once the local stability limit is reached. The path followed by the system depends on the presence

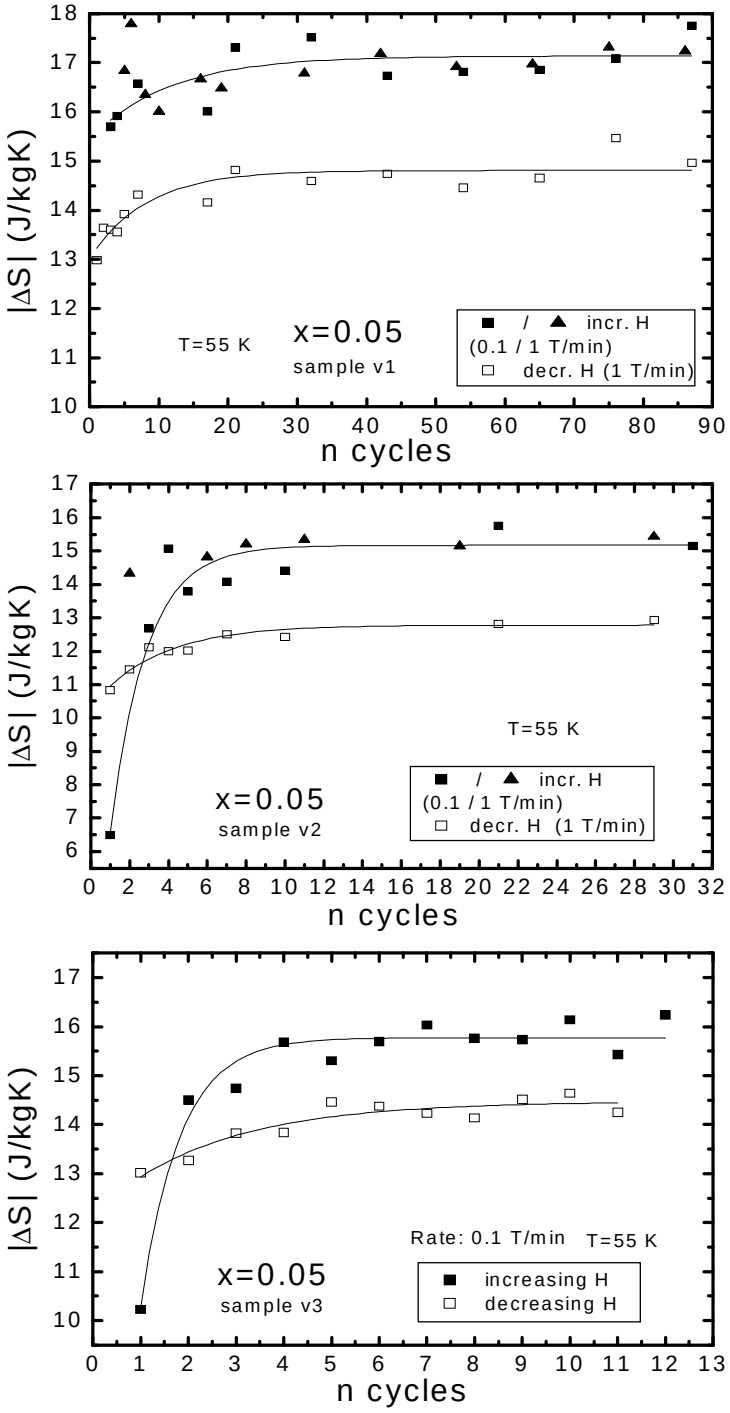

Figure 9.7: Entropy change obtained from $DSC_T(H)$ measurements (increasing and decreasing H at different rates) in samples v1, v2 and v3 (x=0.05), as a function of the number of cycle. Field rates, $\dot{H}$, are given in the plots. Solid lines are a guide to the eye.

of disorder such as dislocations, vacancies or grain boundaries, which controls the distribution of energy barriers separating the two phases. As the system is driven, it passes through a sequence of metastable states with discontinuous steps or avalanches of the order parameter, which reflect the fact that the system jumps from one metastable free energy minimum to another one with an associated energy dissipation, which is responsible for the hysteresis observed in first-order transitions [6]. In the athermal case, the path can be reproduced from cycle to cycle provided that disorder does not evolve [7].

From $DSC_T(H)$ curves obtained on increasing and decreasing H, the transformed fraction of a sample, y, can be evaluated as a function of H as,

$$y(H) = \frac{1}{L}\int_{H_i}^{H} \frac{dQ}{dH} dH \ , \tag{9.9}$$

where $L = \int_{H_i}^{H_f} (dQ/dH)dH$ is the latent heat, and H_i and H_f are magnetic fields above and below the starting and finishing transition fields, respectively. $y(H)$ for increasing and decreasing H enables us to display the hysteresis loops. In order to quantify the amplitude of the jumps in the first-order transition (*i.e.*, structure peaks) present in x=0.05 samples (see Figs. 4.8, 9.5 and 9.6), we computed the difference between two consecutive $y(H)$ values from the experimentally measured dQ/dH curve, which was recorded every 4 s. This difference, Δy, which is a measurement of the size of the avalanches, can vary from 0 (no avalanche event has occurred during the measuring time window) to 1 (the whole system undergoes the transition in a single avalanche event). Figure 9.8 shows a distribution of Δy obtained from $DSC_T(H)$ measurement at cycle 12 in sample v3.

The distribution of avalanches can be statistically analysed using the following probability distribution with two free parameters (λ and α) [8, 9]:

$$p(\Delta y) = \frac{e^{-\lambda \Delta y}(\Delta y)^{-\alpha}}{\int_{\Delta y_{min}}^{\Delta y_{max}} e^{-\lambda \Delta y}(\Delta y)^{-\alpha} d(\Delta y)} \ . \tag{9.10}$$

For λ=0, the distribution is a power law [$p \propto (\Delta y)^{-\alpha}$, a critical behaviour where there is not a characteristic size], while it is subcritical for λ>0 (the distribution decays faster than a power law) and supercritical for λ<0 (the distribution decays slower than a power law) [10]. $\Delta y_{min}=10^{-4}$ is a value just above the intrinsic noise level of the measurements, evaluated by considering Δy values outside the region where the DSC peak shows structure. Δy_{max}=1 is the maximum value.

We have estimated the exponent α and the parameter λ by the maximum likelihood method [11]. This method is the most reliable since it does not involve the computation of histograms, which normally depend on the binning choice. Figure 9.8 shows an example of one of such fits. The fact that samples v1 and v2 do

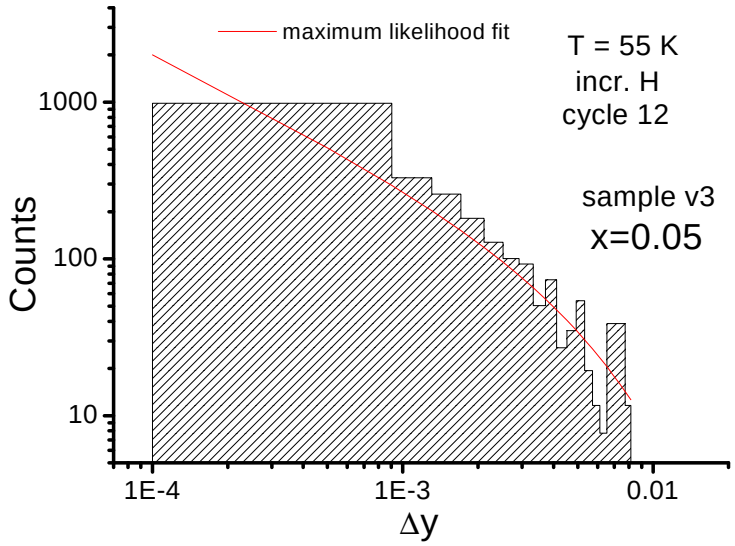

Figure 9.8: Distribution of avalanches obtained from the difference in the transformed fraction (Δy) and the corresponding maximum likelihood fit for one of the measurements (cycle 12) in sample v3.

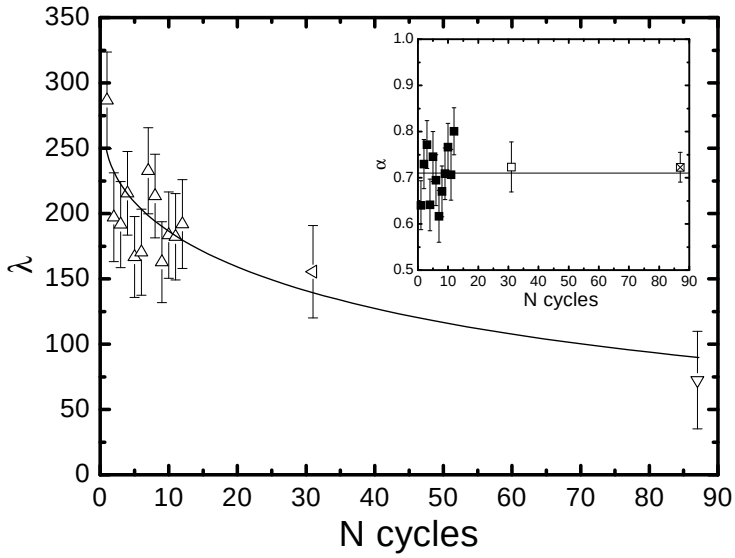

Figure 9.9: Parameter λ obtained from the distribution of avalanches using the transformed fraction of the sample v3 (x=0.05), as a function of the cycle. Cycle 31 is taken from sample v2 and cycle 89 from sample v1. Inset: Exponent α obtained from the same distribution of avalanches. Solid lines are a guide to the eye.

not present a completely systematic cycling (first measurements where recorded at different values of $\dot{H}$ on increasing H) led us to repeat the cycling with sample v3, after we observed that $\dot{H}$=0.1 T/min was optimal taking into account the acquisition rate of the calorimeter, which is 0.25 Hz. This $\dot{H}$ enables us to observe the avalanche structure while the signal of the sensors is large enough to be recorded above noise. Results for increasing H in sample v3 are displayed in Fig. 9.9. We note that the parameter λ tends to decrease with the number of cycles, while the exponent α (inset in Fig. 9.9) remains constant (α=0.71±0.05). We have also added the values fitted for the last cycle of sample v2 (cycle #31) and sample v1 (cycle #89), since those cycles were done with the same field rate as in sample v3. The latter values are in agreement with the behaviour of the two parameters for sample v3. λ and α may also be evaluated from $\mathrm{DSC}_T(H)$ curves shown in Fig. 4.8 in a sample with x = 0.05 cut from the same original button (#1 T4+Q) that samples v1, v2 and v3. The number of cycles previously undergone by this sample was not controlled, although it can be estimated as ~15-25. In this case, α=0.73±0.05 and λ=209±30, in excellent agreement with the previous results (Fig. 9.9).

The evolution of the parameter λ indicates that our system evolves from a subcritical distribution towards a power law distribution (where the system does not have a preferential avalanche size to undergo the transition), although the value λ=0 is not reached in the 89th cycle. The characteristic exponent for the power law, α, presents a value (=0.71±0.05) which neither dependends on the evolution of the system with cycling, nor on the sample. The evolution of the parameters are consistent with previous observations: when the system has chosen a path which is optimal to undergo the transition, both the entropy change and the distribution of avalanches tend towards a constant behaviour.

9.5 Conclusions

The study of dynamics of the first-order transition in $Gd_5(Si_xGe_{1-x})_4$ alloys has unveiled a very interesting behaviour. Our DSC under field has revealed that the entropy change associated with the transition is different when it is field- or thermally-induced, evidencing that the initial and final states are different due to the fact that the transition is not ideal. Cycling through the transition shows that the field-induced entropy change increases for a few cycles, reaching a stationary value. This behaviour is related to the avalanche distribution, which also evolves with cycling. The structure of avalanches becomes repetitive after a few cycles tending towards a power-law distribution, unveiling the athermal character of the magnetostructural transition.

Bibliography

[1] M. W. Zemansky and R. H. Dittman, *Heat and thermodynamics*, 6th ed. (McGraw-Hill, New York, 1981).

[2] E. M. Levin, A. O. Pecharsky, V. K. Pecharsky, and K. A. Gschneidner, Jr., Phys. Rev. B **63**, 064426 (2001).

[3] J. B. Sousa, M. E. Braga, F. C. Correia, F. Carpinteiro, L. Morellon, P. A. Algarabel, and M. R. Ibarra, Phys. Rev. B **67**, 134416 (2003).

[4] J. B. Sousa, M. E. Braga, F. C. Correia, F. Carpinteiro, L. Morellon, P. A. Algarabel, and M. R. Ibarra, J. Appl. Phys. **91**, 4457 (2002).

[5] F. J. Pérez-Reche, E. Vives, L. Mañosa, and A. Planes, Phys. Rev. Lett. **87**, 195701 (2001).

[6] F. J. Pérez-Reche, M. Stipcich, E. Vives, L. Mañosa, A. Planes, and M. Morin, accepted in Phys. Rev. B (unpublished).

[7] J. P. Sethna, K. Dahmen, S. Kartha, J. A. Krumhansl, B. W. Roberts, and J. D. Shore, Phys. Rev. Lett. **70**, 3347 (1993).

[8] E. Vives, J. Ortín, L. Mañosa, I. Ràfols, R. Pérez-Magrané, and A. Planes, Phys. Rev. Lett. **72**, 1694 (1994).

[9] L. Carrillo, L. Mañosa, J. Ortín, A. Planes, and E. Vives, Phys. Rev. Lett. **81**, 1889 (1998).

[10] E. Vives and A. Planes, Phys. Rev. B **50**, 3839 (1994).

[11] R. Barlow, *Statistics* (Wiley, New York, 1989).